

# Results from the Telescope Array Experiment

Charles C. H. Jui<sup>a</sup> for the Telescope Array Collaboration

<sup>a</sup>Department of Physics and Astronomy, University of Utah, 115 S 1400 E JFB 201, Salt Lake City, Utah 84112, U.S.A.

---

## Abstract

The Telescope Array (TA) is the largest ultrahigh energy cosmic ray detector in the northern hemisphere. The experiment consists of three fluorescence stations viewing the air space over a surface array of 507 scintillation counters deployed over 700 square kilometers. TA has been in operation since 2008. The most recent results from TA, including that of composition studies and search for arrival direction anisotropy, will be presented. We will also report on the progress of the new TA low energy extension (TALE).

*Keywords:* particle astrophysics, cosmic rays, energy spectrum, anisotropy, composition, Telescope Array

---

## 1. Introduction

The Telescope Array is the largest experiment studying ultrahigh energy cosmic rays in the northern hemisphere. The project is located near the city of Delta, Utah, U.S.A. The apparatus consists of a surface detector (SD) of 507 scintillation counters arranged in a square grid [1]. The nearest neighbour distance is 1.2km, and the array covers an area of about 730 km<sup>2</sup>. Three fluorescence detectors (FD) look inward from the periphery of the SD array [2]. The arrangement of the detector is shown in Figure 1.

The TA collaboration consists of about 120 members from 30 institutions in Japan, the U.S, Russia, Republic of Korea, and Belgium. The Telescope Array experiment began construction in 2006, and has been in routine operations since 2008. Data from the FD and SD detectors can be analysed separately in SD-only or FD monocular modes. Data can also be combined in stereo mode between FD stations, or in hybrid co incidence mode between FD and SD.

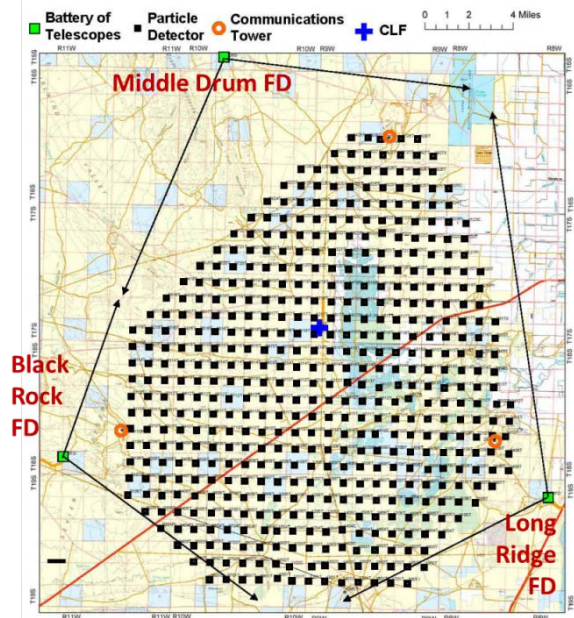


Figure 1: Layout of the Telescope Array experiment. The surface detectors are shown by the black squares and the fluorescence detector stations by the green squares.

## 2. TA detectors

### 2.1. Surface Detector

Each SD counter consists of two layers of plastic scintillators of 1.25cm each in thickness, and 3.0m<sup>2</sup> in total area. Wavelength-shifting optical fibers are embedded in extruded grooves of the plastic to achieve uniform collection of light. The fibers are each bundled into separate photomultiplier tubes (PMTs), one for each layer for readout. The power for the SD stations is provided by solar panels with deep-cycle batteries. Each counter communicates over a 2.4GHz wireless network with one of three communication towers located near the FD stations.

Once every ten minutes, each SD unit runs through a calibration cycle using distribution of pulse heights from minimum-ionizing cosmic muons. The signal from each PMT is digitized at 50Mps. Data is stored for pulses that exceed 0.3 vertical equivalent muons (VEM) in area over background. An array trigger is formed when three adjacent counters report  $\geq 3$  VEM pulses in time coincidence, after which the counters are polled and all stored pulses in the trigger window are transferred to the central data acquisition.

### 2.2. Fluorescence Detector

Each FD station views between 3° and 31° in elevation, and  $\sim 110^\circ$  in azimuth. A total of 38 telescopes are distributed over the three FD stations. The two southern sites at Black Rock Mesa (BRM) and Long Ridge (LR) are equipped with 12 new telescopes constructed in Japan. Each has a segmented spherical mirror of 6.8m<sup>2</sup> in area. The focal plane camera consists of 256 PMT pixels in a 16×16 hexagonal honeycomb structure. Each pixel views approximately a 1.1° cone in the sky. The northern site at Middle Drum (MD) houses 14 telescopes refurbished from HiRes-1 detector site of the High Resolution Fly's Eye (HiRes) Experiment. The FD telescopes operate on clear, moonless nights and accumulate an average of about 10% live time.

### 2.3. Low Energy Extension

In addition to the primary SD array and FD telescopes, the TA collaboration has added a TA low-energy extension (TALE) consisting of ten high elevation telescopes at the MD site, and an infill surface detector array [3]. The new telescopes view between 31 and 59° in elevation, and 80° of azimuth.

The TALE FD was completed in the fall of 2013. The infill SD consists of 75 counters identical to those in the main array. They are arranged in a graded spatial distribution shown in Figure 2. As of summer 2014, 32 SD counters are in place, of which 16 have been instrumented with readout electronics.

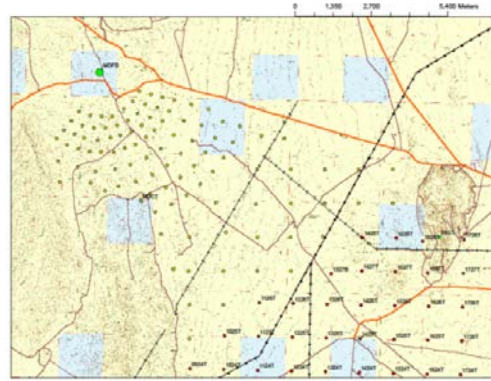


Figure 2: layout of the TALE surface detectors. The Middle Drum (MD) FD site is shown by the square circle in the upper left, and the TALE SD units fan out in a graded pattern to the south of MD. The array shown in the lower right hand of the map are those of the main TA SD array with 1.2km spacing between nearest neighbors.

## 3. Data Analysis

### 3.1. SD Data Analysis

Figure 3 shows a typical high energy event seen by the SD array. The axes show the grid position (1200m spacing) of the hit counters. The size of the circle gives the pulse height, and the color indicates the arrival time. The arrival times are fit to a curved shower front model in order to determine both the arrival direction and the shower core—the location where the shower axis intersects ground.

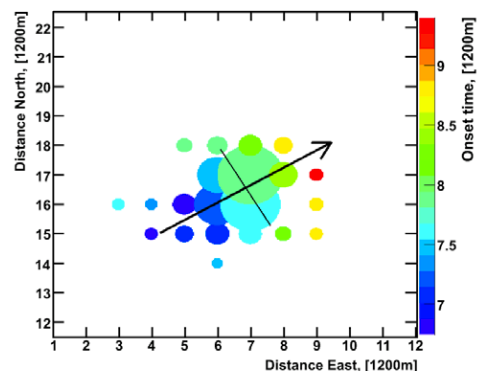


Figure 3: Display of a surface detector event from June 25, 2008. The size of the circles indicates relative particle density seen by each counter in the event. The colors indicate the time of the signal.

Using the trajectory of the shower obtained, the pulse heights are converted to particle densities and plotted against distance perpendicular to the shower axis, as shown in Figure 4. The density at 800m (S800) is interpolated from the fit. Together, S800 and the zenith angle are compared to a look up table to obtain the raw shower energy. This table is constructed from CORSIKA [4] simulations using the QGSJET II hadronic model.

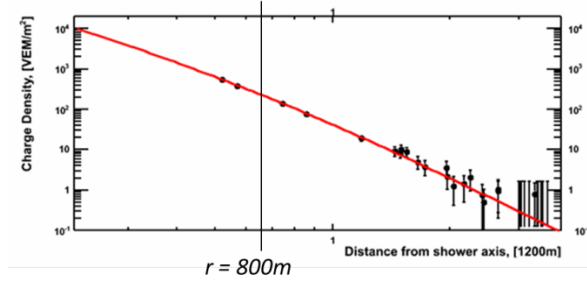


Figure 4: Plot of particle density vs. distance to the shower axis (the lateral density distribution) for the event shown in Figure 3. The density at 800m (S800) is interpolated from the fit, and used with the zenith angle of the shower to obtain the raw shower energy from a look up table.

### 3.2. Hybrid Data Analysis

Figure 5 shows an FD event display, where the signal strength seen by each PMT is indicated by the size of the circle, and the arrival time by the color. A shower-detector plane (SDP) is obtained from the spatial distribution of hit pixels. The shower axis is then fit from the arrival times, including propagation delay of the fluorescence light. This time-fit is illustrated in Figure 6. In this plot, the times of the hit SD counters (with propagation corrections applied) are also included in the fit. The use of the SD information makes this a hybrid time fit, which can achieve angular resolutions of  $\sim 0.6^\circ$ , compared to  $\sim 4^\circ$  for monocular, FD only time fit.

With the known shower trajectory, the pointing direction of each pixel can be converted to an atmospheric slant depth,  $X$ . The signal strength vs. depth for this event is shown in Figure 7. The signal profile is fitted to a shower profile (number of charged particles in shower vs. depth). This fit accounts scintillation (fluorescence) light as well as direct and indirect Cherenkov light. The energy of the shower is then obtained from the integral of the shower profile, whereas the depth of the shower maximum ( $X_{\max}$ ) gives a statistical measure of the composition of the primary cosmic rays.

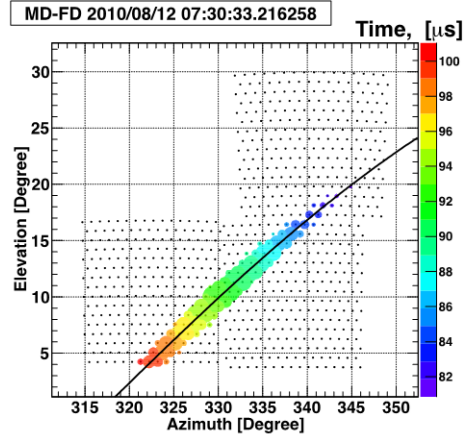


Figure 5: Event display of an FD event from the Middle Drum site. The circles indicate hit PMT pixels. The size of the circles gives the signal strength, while the colors indicate arrival times. The solid curve gives the fitted shower-detector plane.

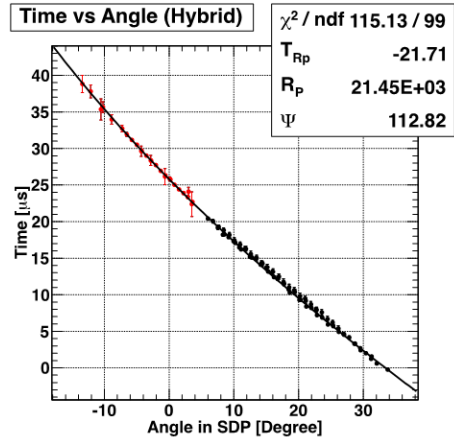


Figure 6: Plot of signal arrival time for FD pixels (black points) vs. the angle measured from the horizon to the pixel, along the shower-detector plane (SDP). This fit is made an order of magnitude more precise by the inclusion of the times of the SD hits (red points).

## 4. Results

### 4.1. SD Energy Scale

One of the first results from TA was obtained by correlating the SD-only and hybrid FD results, where we observed the SD to yield a 27% higher energy than that by the hybrid FD analysis for the same events. This offset appears to be independent of energy, as seen in Figure 8. This scale shift may account for the difference in normalization between the UHECR flux obtained by AGASA (SD) [5] and that from the HiRes experiment (FD) [6].

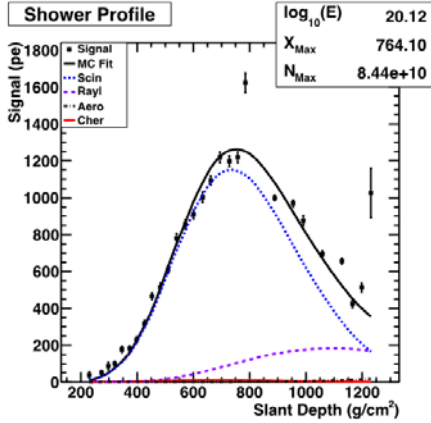


Figure 7: Signal vs. depth for the hybrid FD event shown in Figure 5 and Figure 6. The black curve shows the overall fit to the data, where the blue dotted curve gives the contribution of the scintillation (fluorescence) light, and the purple dash gives the Rayleigh-scattered Cherenkov, and the solid red curve the direct Cherenkov light.

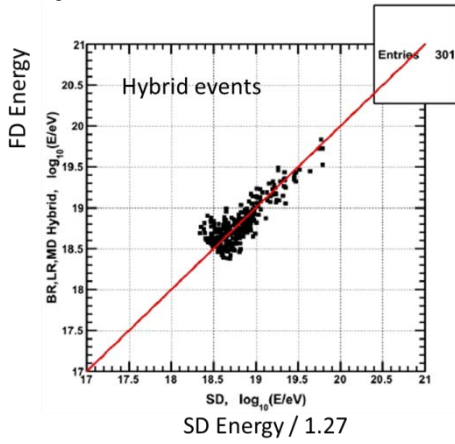


Figure 8: Scatterplot of FD energy from hybrid events vs. rescaled SD energies (divided by 1.27) for the same events. The 27% offset appears uniform over the energy range  $10^{18.5}$ - $10^{20}$  eV.

#### 4.2. Energy Spectrum

After correcting the SD energies to that of the FD, we obtained an UHECR energy spectrum in excellent agreement with previously reported HiRes results, in normalization, in the location of the ankle/dip structure at  $\sim 10^{18.6}$  eV, and in the observation of the Greisen-Zatsepin-K'uzmin (GZK) [7,8] suppression at  $\sim 10^{19.8}$  eV. The TA result, from five years of SD data, is shown in Figure 9. Results from HiRes, AGASA [5], and Auger [9] are also shown for comparison. This spectrum is an update of the published result based on the first four years of data [10]. The significance of the GZK suppression has been improved to  $5.7\sigma$ .

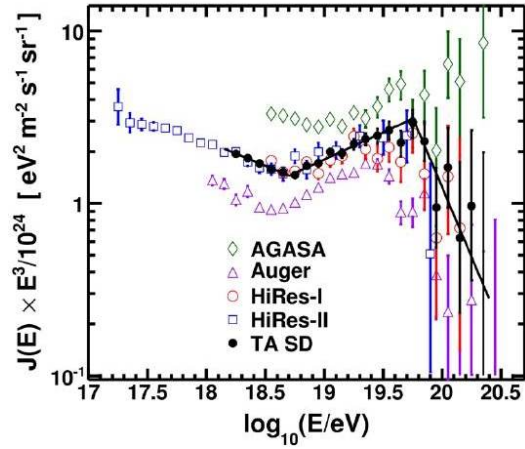


Figure 9: UHECR flux ( $\times E^3$ ) vs  $\log E$  (eV) from five years of TA SD data overlaid with results from HiRes [6], AGASA [5], and Auger [9].

#### 4.3. Composition

TA has performed composition studies in both stereo and in hybrid mode. The  $X_{\max}$  vs  $\log E$  plot from the first five years of TA stereo analysis is shown in Figure 10 [11]. A similar plot from the hybrid FD analysis is given in Figure 11 [12]. In both figures, the red and blue lines give predictions for proton and iron from simulation. The TA measurements are consistent with light composition.

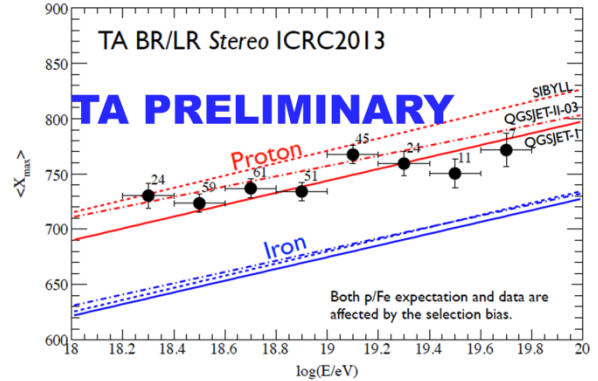


Figure 10: Average  $X_{\max}$  vs.  $\log E$  plot from stereoscopic FD analysis from the first five years of TA data. Predictions of shower simulations for pure proton and iron are shown in red and blue, respectively. TA results are consistent with light composition.

#### 4.4. Anisotropy

Until recently, the TA collaboration has reported no significant signals in our search for anisotropy in the arrival direction of UHECR induced air showers (see,

for exmaple, reference [13]). However, a new publication shows a very tantalizing result [14].

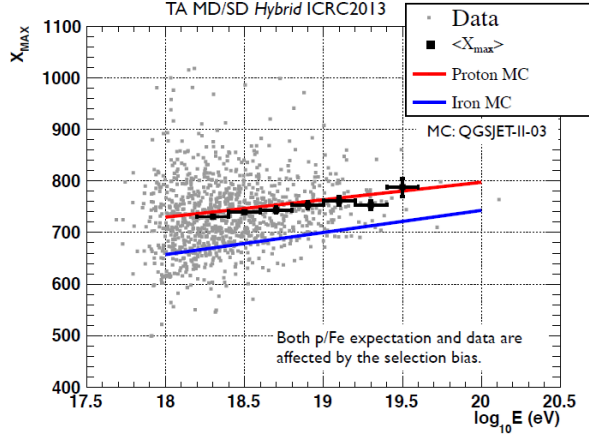


Figure 11: Average  $X_{\max}$  vs.  $\text{Log}E$  plot from hybrid FD analysis. Predictions of shower simulations for pure proton and iron are shown in red and blue, respectively. TA results are consistent with light composition

Figure 12 shows the arrival direction of the highest energy events ( $E > 5.7 \times 10^{19} \text{eV}$ ) detected by the TA surface detector over the first five years of observation. The threshold energy of  $5.7 \times 10^{19} \text{eV}$  is an *a priori* selection following the hypothesis of AGN correlations claimed previously by the Pierre Auger Observatory [15]. Visual inspection of the sky map shows an apparent excess of events at  $\text{R.A.} \approx 150^\circ$ ,  $\text{DEC} \approx +40^\circ$ .

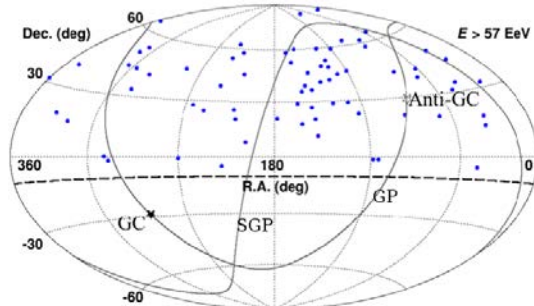


Figure 12: Arrival directions of TA SD events, shown with blue dots, with energy in excess of  $5.7 \times 10^{19} \text{eV}$ . The plot is made in equatorial coordinates.

A statistical test was applied where the data were oversampled successively in cones of  $15^\circ$ ,  $20^\circ$ ,  $25^\circ$ ,  $30^\circ$ , and  $35^\circ$  (half angle), and compared to the expectations from one million sets of 72 MC events simulated according to an isotropic source distribution. The centers of the cones are varied in  $0.1^\circ$  steps in both R.A. and DEC. We found a

maximum local excess of  $5.1\sigma$  (19 data events over an expected background of 4.2) in a  $20^\circ$  cone centered at  $\text{R.A.} = 146.7^\circ$ ,  $\text{Dec.} = 43.2^\circ$ . The result of this search for the  $20^\circ$  case is shown in Figure 13.

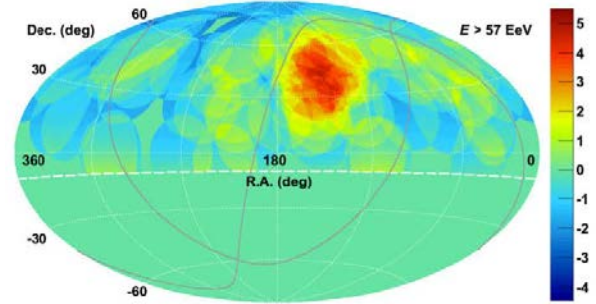


Figure 13: Local excess significance of oversampling in  $20^\circ$  (half-angle) cones of the sky of data points from Figure 12, compared to expectations averaged from one million simulated data sets of 72 events drawn from an isotropic source distribution. The results are shown for centers of R.A. and DEC in  $0.1^\circ$  intervals.

The  $5.1\sigma$  represents the significance of the excess in data events in that particular cone over isotropic background, whereas the global significance of the apparent clustering must be estimated from the fraction of MC sets that shows an excess somewhere in the field of view of  $5.1\sigma$  or greater. From the one million simulated event sets we find the probability of greater local excess (for all five cone angles searched) to be  $p = 3.7 \times 10^{-4}$ , or about  $3.4\sigma$ .

#### 4.5. Results from TALE

The ten TALE telescopes have been taking data since the fall of 2013. The analysis has thus far concentrated on measuring the energy spectrum using only data from the ten new telescopes. The primary goal of these early studies is to verify the energy scale and efficiency of the FD. Figure 14 shows the preliminary spectrum from TALE.

The original design of TALE was to lower the energy threshold for physics down to  $10^{16.5} \text{eV}$ . The black points in the figure show the spectrum obtained from the conventional event selection for cosmic ray showers cutting out Cherenkov-light dominated events. However, a new analysis method developed to reconstruct Cherenkov-dominated event allowed us to extend the threshold energy down nearly another order of magnitude. These results are shown by the red data points in Figure 14. The two TALE spectra agree well in the overlap region with one another, and the upper end is consistent with previously results from HiRes-2 and HiRes-MIA.

The aperture calculation for TALE becomes very sensitive to composition at below  $10^{17}$  eV. We have assumed a mixed composition proposed by Gaisser in this analysis [16].

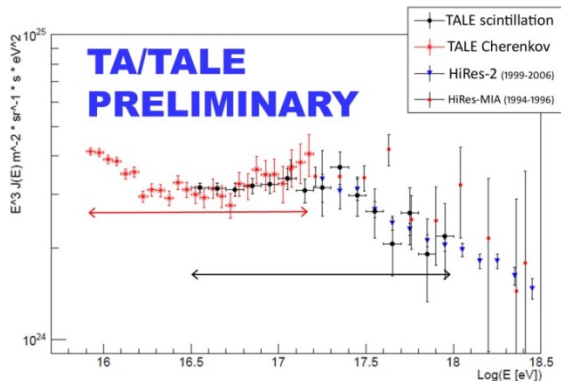


Figure 14: Preliminary monocular energy spectrum using data from the ten new TALE high-elevation telescopes only. The black data points show the spectrum of events analyzed from primarily scintillation (fluorescence) light. The red points show the spectrum from the analysis of Cherenkov-light dominated events. Previous spectra from HiRes-2 and HiRes-MIA are also shown.

## Acknowledgments

The Telescope Array experiment is supported by the Japan Society for the Promotion of Science through Grants-in-Aids for Scientific Research on Specially Promoted Research (21000002) “Extreme Phenomena in the Universe Explored by Highest Energy Cosmic Rays” and for Scientific Research(19104006), and the Inter-University Research Program of the Institute for Cosmic Ray Research; by the U.S. National Science Foundation awards PHY-0307098, PHY-0601915, PHY-0649681, PHY-0703893, PHY-0758342, PHY-0848320, PHY-1069280, and PHY-1069286; by the National Research Foundation of Korea (2007-0093860, R32-10130, 2012R1A1A2008381, 2013004883); by the Russian Academy of Sciences, RFBR grants 11-02-01528a and 13-02-01311a (INR), IISN project No. 4.4509.10 and Belgian Science Policy under IUAP VII/37 (ULB). The foundations of Dr. Ezekiel R. and Edna Wattis Duke, Willard L. Eccles and the George S. and Dolores Dore Eccles all helped with generous donations. The State of Utah supported the project through its Economic Development Board, and the University of Utah through the Office of the Vice President for Research. The experimental site became available through the cooperation of the Utah School and Institutional Trust Lands Administration (SITLA),

U.S. Bureau of Land Management, and the U.S. Air Force. We also wish to thank the people and the officials of Millard County, Utah for their steadfast and warm support. We gratefully acknowledge the contributions from the technical staffs of our home institutions. An allocation of computer time from the Center for High Performance Computing at the University of Utah is gratefully acknowledged.

## References

- [1] T. Abu-Zayyad *et al.* (TA Collaboration), Nucl. Instr. Meth. **A689** (2012) 87–97.
- [2] H. Tokuno *et al.* (TA Collaboration), Nucl. Instr. Meth. **A676** (2012) 54–65.
- [3] S. Ogio for the TA Collaboration, Proc. 33<sup>rd</sup> ICRC, Rio de Janeiro, 2013 #717.
- [4] D. Heck *et al.* Forschungszentrum Karlsruhe Report FZKA 6019 (1998).
- [5] M. Takeda *et al.*, Astropart. Phys. **19** (2003) 447.
- [6] R. U. Abbasi *et al.* (High Resolution Fly’s Eye Collaboration), Phys. Rev. Lett. 100 (2008) 101101.
- [7] K. Greisen, Phys. Rev. Lett. **16** (1966) 748.
- [8] Zatsepin, G.T. and V.A. K’uzmin, Pis’ma Zh. Eksp. Teor. Fiz., **4** (1966.) 114; [ JETP Lett. **4** (1966) 78. ]
- [9] Abraham, J., *et al.* Phys. Lett., **B685**, (2010) 239.
- [10] T. Abu-Zayyad *et al.* (TA Collaboration), ApJ **768** (2013) L1.
- [11] Y. Tameda for the TA Collaboration, Proc. 33<sup>rd</sup> ICRC, Rio de Janeiro, 2013 #512.
- [12] M. Allen for the TA Collaboration, Proc. 33<sup>rd</sup> ICRC, Rio de Janeiro, 2013 #794.
- [13] T. Abu-Zayyad *et al.* (TA Collaboration), ApJ **777** (2013) 88.
- [14] R.U. Abbasi *et al.* (TA Collaboration), ApJ **790** (2014) L21.
- [15] The Pierre Auger Collaboration, Science **318** (2007) 938.
- [16] T.K. Gaisser, Astropart.Phys. **35** (2012) 801.